Int. J. Nanosci. Nanotechnol., Vol. 12, No. 3, Sept. 2016, pp. 139-147

-OSO_3H Functionalized Mesoporous MCM-41 Coated on Fe_3O_4 Nanoparticles: an Efficient and Recyclable Nano-Catalyst for Preparation of 3,2′-Bisindoles

Alireza Khorshidi[1]* and Shahab Shariati[2]

[1]Department of Chemistry, Faculty of Sciences, University of Guilan, P.O.Box 41335-1914, Rasht, Iran
[2]Department of Chemistry, Faculty of Science, Rasht Branch, Islamic Azad University, Rasht, Iran

(*) Corresponding author: Khorshidi@guilan.ac.ir
(Received: 20 August 2015 and Accepted: 03 July 2016)

Abstract

Mesoporous MCM-41 was coated on Fe_3O_4 nanoparticles and then functionalized with sulfurochloridic acid to provide a core-shell solid acid nano-catalyst. The catalyst was characterized by transmission electron microscopy (TEM), infrared spectroscopy (FTIR), X-ray diffraction (XRD), thermogravimetric analysis (TG), Brunauer-Emmet-Teller analysis (BET) and vibrating sample magnetometery (VSM). The obtained nano-sized magnetic catalyst was used in three-component reaction of indoles, phenylglyoxal monohydrate and N-arylenaminones to furnish the desired 3,2′-bisindoles in good yields under mild reaction conditions. In order to evaluate reusability of the catalyst, the reaction of indole, phenylglyoxal monohydrate and 5,5-dimethyl-3-(phenylamino)cyclohex-2-enone was carried out in the presence of the recycled catalyst in successive runs. From reaction run 1 to 5, the yields were 89%, 89%, 81%, 75% and 63%, respectively. Therefore after five runs, 26% decrease in the efficiency of the catalyst system was observed. In order to confirm heterogeneity of the catalyst, the amount of sulfonic acid loading was determined for the recycled catalyst of the 3rd run and a similar result (2.40 mmol SO_3H/g) was obtained, which confirmed that no considerable leaching was occurred during the course of reaction.

Keywords: *3,2′-bisindole, Core-shell, Heterogeneous, Solid acid, Catalyst.*

1. INRODUCTION

Fascinating properties of indoles have attracted attention for many years [1, 2]. Indole ring is embedded in a myriad of pharmacologically and biologically active compounds [3]. For example, indirubin (Figure 1) as a 3,2′-bisindole derivative acts as cyclin-dependent kinase inhibitor and dioxin receptor [4-6].

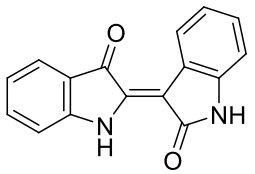

Figure 1. *Indirubin*

Thus far, most studies have been focused on functionalization of the most nucleophilic site of the molecule (C-3), and a huge number of works on preparation of 3-substituted indoles, especially 3,3′-bis(indolyl)methanes, have been reported [7]. Little attention has been paid, however, to the multicomponent reactions which involve all three nucleophilic centers of the indole ring system. Some exciting reports in this context include Jiang's works on multicomponent domino reactions resulting in polyfunctionalized indole [8-10]. We have been involved in the study of

indoles and solid acid catalysts [11-13], and a recent report on three-component formation of bis-indole derivatives by Fu [14], encouraged us to investigate application of acid-functionalized magnetic nanoparticles to improve such a reaction with respect to the catalyst loading, reaction time, and above all, recovery and reuse of the catalyst which reduces environmental concerns and paves the way for scale-up usage. Mesoporous materials such as MCM-41 on the other hand, have been studied extensively thus far [15, 16]. Hereby, we introduce –OSO_3H functionalized MCM-41 coated on Fe_3O_4 nanoparticles (Fe_3O_4@MCM-41-OSO_3H) as an efficient solid acid catalyst for three component reaction of indoles, phenylglyoxal monohydrate and *N*-arylenaminones under mild reaction conditions (Scheme 1). A unique feature of the catalyst is that it could be easily separated from the reaction mixture by an external magnet.

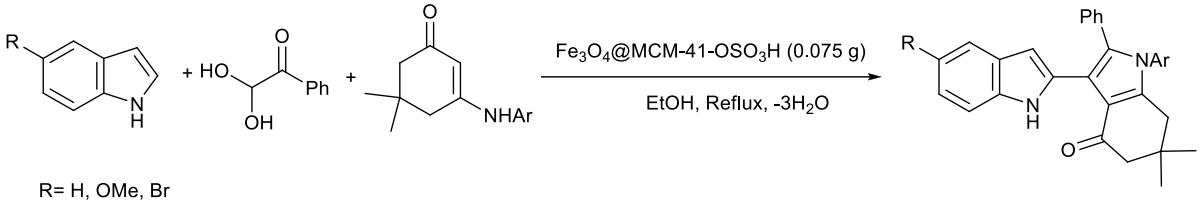

R= H, OMe, Br
Ar= C_6H_5, 4-ClC_6H_4, 4-BrC_6H_4, 4-MeC_6H_4, 4-$MeOC_6H_4$

Scheme 1. *Fe_3O_4@MCM-41-OSO_3H catalyzed three component regioselective synthesis of 3,2'-bisindoles*

2. EXPERIMENTAL

2.1. Materials

Caution: $ClSO_3H$ is fuming and irritant. Precautions, such as proper ventilation, should be observed. Fe_3O_4 magnetite nanoparticles were synthesized according to the literature [17]. For the synthesis of Fe_3O_4@MCM-41, 1.5 g of the synthesized Fe_3O_4 nanoparticles were dispersed in a mixture of ammonia solution (5 mL, 25%) and distilled water (50 mL) in a glass reactor by using ultrasound irradiation for 2 min at 40 °C. Then, tetraethylorthosilicate (TEOS, 10.0 mL), NaOH (0.9 g) and NaF (0.19 g) were added to the mixture and stirred for 2 h prior to addition of Cetyltrimethylammonium bromide (CTAB, 7.0 g). The mixture was then stirred at 40 °C for 2 h. At the end of this process, the magnetic composite was hydrothermally treated at 120 °C for 48 h in an autoclave. After two days, the resultant solid was filtered, washed with distilled water and dried at 60 °C. Finally, the template was removed by calcination of the synthesized particles for 3 h at 300 °C. SO_3H functionalization on Fe_3O_4@MCM-41 was carried out according our previous report .[16] In brief, Fe_3O_4@MCM-41 (2.0 g) was charged into a suction flask equipped with a constant pressure dropping funnel, and dispersed by ultrasound for 10 min in dichloromethane (75 mL). Sulfurochloridic acid (2.92 g, 25 mmol) in CH_2Cl_2 (20 mL) was added dropwise over a period of 30 min at room temperature. The mixture was then stirred for 90 min, while evolving HCl was eliminated by suction. Then the Fe_3O_4@MCM-41-OSO_3H was separated from the reaction mixture by an external magnet and washed several times with CH_2Cl_2, then dried under vacuum at 60 ˚C. The amount of sulfonic acid loading was determined as 2.43 mmol SO_3H/g of the catalyst according to the literature [18].

2.2 Instrumentation

X-ray powder diffraction (XRD) measurements were performed using a Philips diffractometer with mono chromatized Cu k_α radiation. IR spectra were recorded on a Shimadzu FTIR-8400S spectrometer. ^{1}H NMR spectra were obtained on a Bruker DRX-400 Avance spectrometer and ^{13}C NMR spectra were obtained on a Bruker DRX-100 Avance spectrometer. Chemical shifts of ^{1}H and

^{13}C NMR spectra were expressed in ppm downfield from tetramethylsilane. Melting points were measured on a Büchi Melting Point B-540 instrument and are uncorrected. Elemental analyses were made by a Carlo-Erba EA1110 CNNO-S analyzer and agreed with the calculated values. TEM images were obtained on a transmission electron microscope (TEM-PHILIPS MC 10) with an acceleration voltage of 80 kV. VSM curves were obtained on a vibrating sample magnetometer (VSM JDM-13) at room temperature. Analytical GC evaluations of product mixtures were carried out on a Teif Gostar Faraz GC-Chrom, Iran (using a split/splitless injector, CP Sil 8CB column, FID assembly).

2.3. Typical procedure for the preparation of 3,2′-bisindoles 1a-m.

In a three necked round-bottom flask equipped with a reflux condenser, indole (1.00 mmol), phenylglyoxal monohydrate (1.00 mmol), and *N*-arylenaminone (1.00 mmol) were dissolved in refluxing ethanol (10 mL) and then Fe_3O_4@MCM-41-OSO_3H (0.075 g) was added and the resulting mixture was mechanically stirred until the disappearance of the starting indole was complete (monitored by TLC). After completion of the reaction, the catalyst was removed by an external magnet. The obtained hot solution was quenched with water, and the solidified product was filtered and rinsed with a cold mixture of ethanol and water (70:30), then subjected to a high vacuum overnight, to provide pure product. The recovered catalyst was washed three times with dichloromethane and then dried under vacuum at 60 ^{o}C overnight.

2.4. Characterization data

All of the products are known compounds, and their spectroscopic and physical data, were found to be identical to those described in the literature [18].

3. RESULTS AND DISCUSSION

Mesoporous MCM-41 was used as a shell for Fe_3O_4 magnetic nanoparticles because of its well-defined channel system and higher external hydroxyl groups. Deposition of the shell on the surface of Fe_3O_4 nanoparticles was performed by a convenient and low cost method. Then, simple treatment of the core-shell nanocomposite and sulfurochloridic acid in CH_2Cl_2 provided the solid acid catalyst (Fe_3O_4@MCM-41-OSO_3H) which was characterized by FT-IR, TEM, XRD, TG, BET and VSM techniques. FT-IR spectrum of Fe_3O_4@MCM-41 (Figure 2a) showed characteristic bands of both Fe_3O_4 and mesoporous MCM-41. In the FT-IR spectra of Fe_3O_4@MCM-41-OSO_3H (Figure 2b), basic characteristic vibrations of Fe-O at 588 cm^{-1} and asymmetric stretching, symmetric stretching and bending vibrations of Si-O-Si at 1072, 795 and 453 cm^{-1} were observed. Sulfonyl groups showed their characteristic bands at 1229 cm^{-1} and 1120 cm^{-1}, along with simultaneous disappearance of Si-OH group peak at 900 cm^{-1} [18].

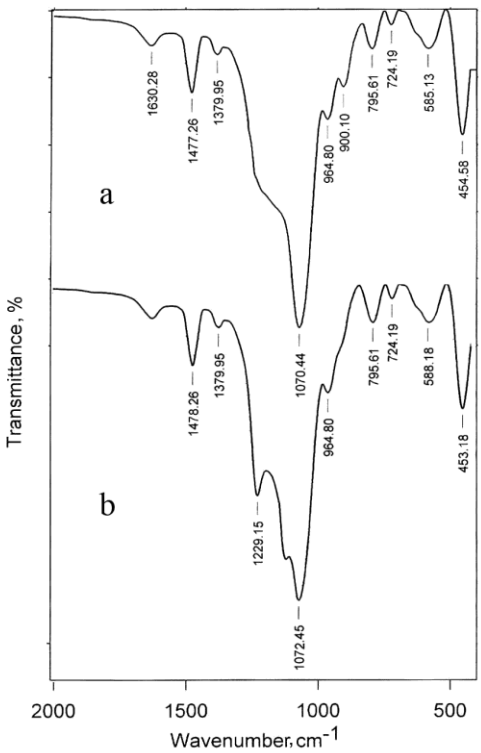

***Figure 2**. FT-IR spectra of a) Fe_3O_4@MCM-41 and b) Fe_3O_4@MCM-41-OSO_3H*

X-ray diffraction (XRD) pattern of Fe_3O_4@MCM-41-OSO_3H (Figure 3) showed peaks that could be indexed to both mesoporous structure and Fe_3O_4 nanoparticles. The Fe_3O_4 nanoparticles indicated peaks with 2θ at 29.72, 35.57, 43.17, 53.44, 57.15 and 62.77, quite identical to pure magnetite (JCPDS No. 19-692) [19]. The smoothly varying peak at 2θ about 20 may be resulted from simultaneous formation of some amorphous silica. The siliceous mesoporous structure, however, indicated peaks with 2θ at 1.5-10 or reflection from the 100, 110 and 200 crystallographic planes, which are characteristic peaks of MCM-41 [20].

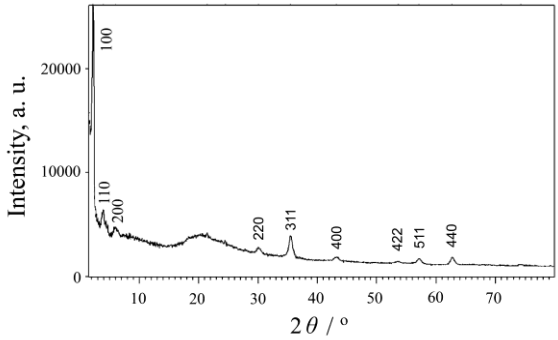

Figure 3. *XRD pattern of Fe_3O_4@MCM-41-OSO_3H nanoparticles*

Transmission electron microscopy (TEM, Figure 4), on the other hand, showed agglomeration of many ultrafine spherical-like particles which display dark magnetite cores surrounded by a mesoporous shell and the channels were almost not occluded. Particle size distribution analysis showed a narrow distribution of particle size about 20 nm.

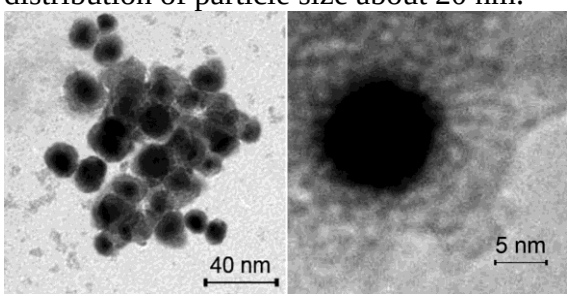

Figure 4. *TEM images of Fe_3O_4@MCM-41-OSO_3H nanoparticles*

Hysteresis curves of the magnetic nanoparticles as a function of applied magnetic field at 300 K were also, obtained (Figure 5). Bare Fe_3O_4 and Fe_3O_4@MCM-41-OSO_3H nanoparticles exhibited typical super paramagnetic behavior. Coating with non-magnetic mesoporous hybrid resulted in decrease of large saturation magnetization of bare Fe_3O_4 from 82 emu.g^{-1} to 45 emu.g^{-1}.

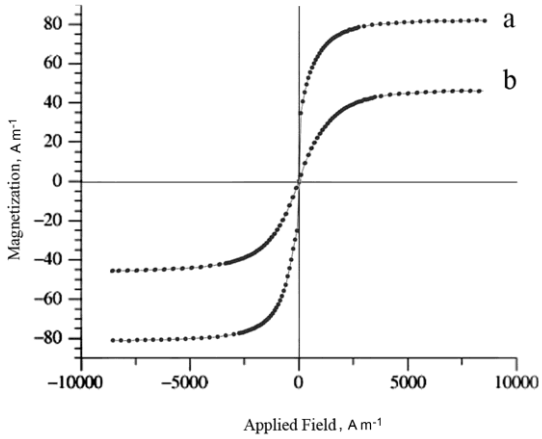

Figure 5. *Hysteresis curves of a) Fe_3O_4 and b) Fe_3O_4@MCM-41-OSO_3H nanoparticles measured at 300 K.*

In addition, mesoporosity of the Fe_3O_4@MCM-41-OSO_3H nanoparticles was evaluated by nitrogen adsorption–desorption isotherms which showed a characteristic type IV curve (Figure 6) with a distinct hysteresis loop in the p/p_0 range of about 0.3, indicating the presence of a narrow distribution of mesoporous pore size.

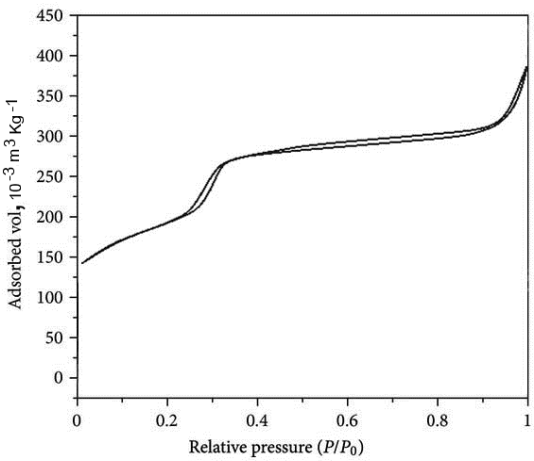

Figure 6. *Nitrogen adsorption-desorption isotherms measured at 77 K for the core–*

shell structured Fe_3O_4@MCM-41-OSO_3H nanoparticles.

Other physico-chemical properties of the Fe_3O_4@MCM-41-OSO_3H nanoparticles are listed in Table 1.

***Table 1**. Physico-chemical properties of the synthesized Fe_3O_4@MCM-41-OSO_3H nanoparticles*

BET surface area (m^2g^{-1})	358.5
Mean pore diameter (BJH)	28 Å
Total pore volume (cm^3g^{-1})	0.401
Mean pore volume (cm^3g^{-1})	0.389

Thermogravimetric (TG) analysis of the catalyst (Figure 7) showed three distinct parts: a) Loss of physisorbed water from 80 to 180 ºC, corresponding to the water molecules absorbed on the external surface and those hosted in the pores, b) loss of template molecules from 200 to 350 ºC and c) collapsing of the –SO_3H functional groups or condensation of silanol groups from 350 to 600 ºC. It may be concluded that the obtained catalyst has enough thermal stability to endure harsh reaction conditions up to 300 ºC.

Acid content of the catalyst was determined according to the literature [18] and a loading of 2.43 mmol –OSO_3H per g of the solid acid catalyst was found. Potentiometric back-titration of the solid acid catalyst, further confirmed this result.

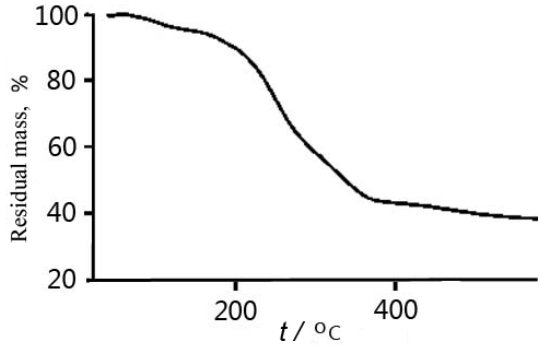

***Figure 7.** TG curve for the Fe_3O_4@MCM-41-OSO_3H nanoparticles obtained in a nitrogen atmosphere at a heating rate of 10 ºC min^{-1}.*

The characterized catalyst, then, was used in one-pot three component condensation reaction of indoles, phenylglyoxal monohydrate and *N*-arylenaminones. In order to optimize the reaction conditions, indole, phenylglyoxal monohydrate and 5,5-dimethyl-3-(phenylamino)cyclohex-2-enone were used as model substrates and their reaction was tested under different conditions. The results are summarized in Table 2.

***Table 2.** Optimization of the three component reaction of indole, phenylglyoxal monohydrate and 5,5-dimethyl-3-(phenylamino)cyclohex-2-enone.*

Entry [a]	Catalyst	Solvent	Catalyst loading (g/mmol of aldehyde)	t / ºC	Yield , %
1	No catalyst	EtOH	0	25	0
2	Fe_3O_4	EtOH	0.075	25	0
3	MCM-41	EtOH	0.075	25	5
4	MCM-41-OSO_3H	EtOH	0.075	25	18
5	Fe_3O_4@MCM-41-OSO_3H	EtOH	0.050	25	16
6	Fe_3O_4@MCM-41-OSO_3H	EtOH	0.075	25	23
7	Fe_3O_4@MCM-41-OSO_3H	EtOH	0.100	25	22
8	Fe_3O_4@MCM-41-OSO_3H	EtOH	0.075	Reflux	89
9	Fe_3O_4@MCM-41-OSO_3H	MeOH	0.075	Reflux	83
10	Fe_3O_4@MCM-41-OSO_3H	1,4-Dioxane	0.075	Reflux	59
11	Fe_3O_4@MCM-41-OSO_3H	1,2-DCE	0.075	Reflux	21
12	Fe_3O_4@MCM-41-OSO_3H	Toluene	0.075	Reflux	15

[a] The reaction was carried out according to general experimental procedure

As it is shown, in the absence of catalyst, the desired product was not formed (entry 1). Although far from ideal, it was proved that Fe_3O_4@MCM-41-OSO_3H in an optimum loading of 0.075 g per mmol of indole (entry 6) is the best choice. MCM-41 sulfuric acid (entry 4) was also tested and the yield was comparable. Fe_3O_4@MCM-41-OSO_3H, however, had the advantage of easy recycling. Higher loads of the catalyst, on the other hand, did not improve the yield (entry 7). Eventually, it was found that elevated temperature has a powerful effect on the reaction yield, and under reflux condition excellent yield of 89% was obtained (entry 8). The yield of the product on the other hand, was solvent dependent and the best solvent was found to be ethanol. After obtaining the optimum reaction condition (Scheme 1), a series of indoles, phenylglyoxal monohydrate and *N*-arylenaminones were used to investigate the generality and scope of the reaction (Table 3) and the results were satisfying, since the same regioselectivity toward 3,2′-bisindoles was observed in each case.

Table 3. *Fe_3O_4@MCM-41-OSO_3H nanoparticles catalyzed regioselective synthesis of 3,2′-bisindoles*

Entry [a]	Indole	Ar	product	Time (min), Yield [b] %
1	Indole	C_6H_5	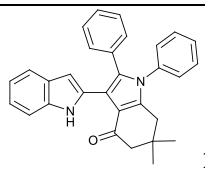 **1a**	45, 89
2	Indole	4-MeC_6H_4	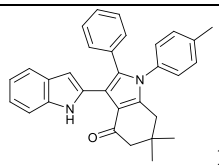 **1b**	40, 90
3	Indole	4-ClC_6H_4	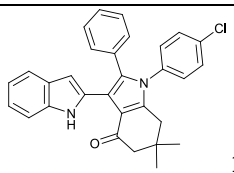 **1c**	50, 79
4	Indole	4-BrC_6H_4	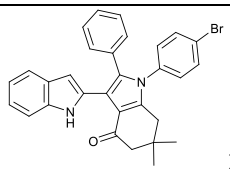 **1d**	30, 86
5	Indole	4-$MeOC_6H_4$	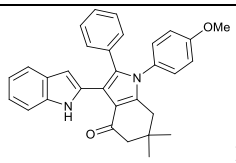 **1e**	20, 88

6	5-Methoxyindole	4-MeC_6H_4	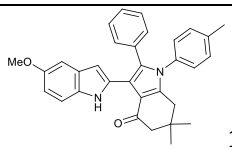 **1f**	25, 87
7	5-Methoxyindole	4-$MeOC_6H_4$	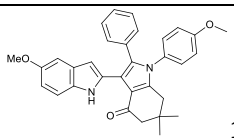 **1g**	20, 92
8	5-bromoindole	C_6H_5	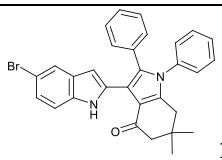 **1h**	30, 79
9	5-bromoindole	4-MeC_6H_4	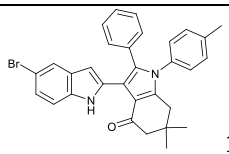 **1i**	35, 90
10	5-bromoindole	4-$MeOC_6H_4$	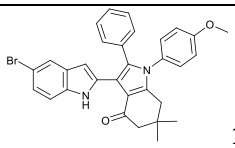 **1j**	35, 91
11	5-bromoindole	4-$ClOC_6H_4$	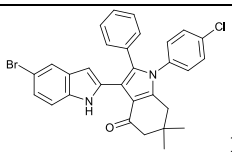 **1k**	55, 86
12	5-bromoindole	4-$BrOC_6H_4$	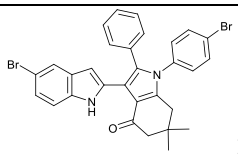 **1l**	25, 93
13	1-methylindole	C_6H_5	**No reaction**	60, 0

[a] All products were characterized by ^{1}H NMR, ^{13}C NMR and IR data; [b] Isolated yields.

As shown in Table 3, various indoles and *N*-arylenaminones participated in the reaction and this catalytic system tolerated different functional groups. 7-azaindole also, participated in this reaction without intervention of N-7 (entry 13). With regard to substituents, electron-releasing nature of the aryl moiety in *N*-arylenaminones favors the formation of products. 1-methylindole, on the other hand, did not yield the desired product. These factors may originate from the reaction mechanism, which we propose as follows (Scheme 2).

In general, after activation of phenylglyoxal monohydrate by the solid Brønsted acid catalyst, nucleophilic attack from C-3 or C-2 carbon atom of indole gives intermediates **I** or **II.** By virtue of the hydrogen bonding between indole NH and the C=O moiety of adduct, **II** is more favored in spite of higher nucleophilicity of C-3. Subsequent nucleophilic attack by β-C atom and NH group of β-enaminone

for C-C and C-N bond formation via [3+2] cyclization, provides intermediate **III**, which finally dehydrates to the product.

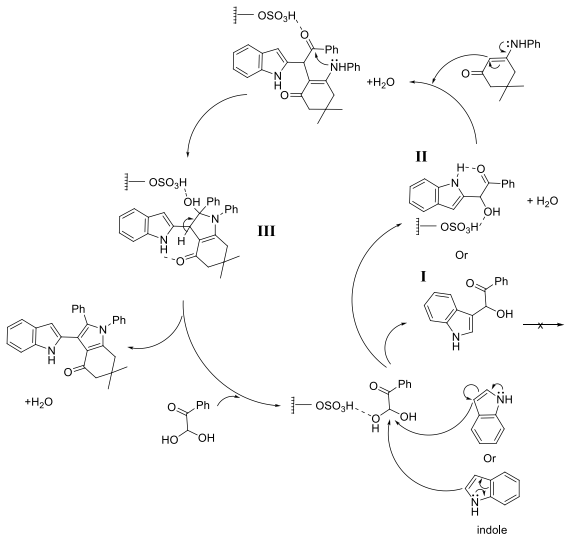

Scheme 2**. A proposed mechanistic pathway for the formation of **1a

In order to evaluate reusability of the catalyst, the reaction of indole, phenylglyoxal monohydrate and 5,5-dimethyl-3-(phenylamino)cyclohex-2-enone was carried out in the presence of the recycled catalyst in successive runs. From reaction run 1 to 5, the yields were 89%, 89%, 81%, 75% and 63%, respectively. Therefore after five runs, 26% decrease in the efficiency of the catalyst system was observed. This result shows that Fe_3O_4@MCM-41-OSO_3H can be utilized as a moderate and recyclable catalyst for the formation of 3,2′-bisindoles. In order to confirm heterogeneity of the catalyst, the amount of sulfonic acid loading was determined for the recycled catalyst of the 3rd run and a similar result (2.40 mmol SO_3H/g) was obtained, which confirmed that no considerable leaching was occurred during the course of reaction. To further approve this assumption, the reaction of indole, phenylglyoxal monohydrate and 5,5-dimethyl-3-(phenylamino)cyclohex-2-enone was interrupted halfway (22.5 min) and the catalyst was removed by an external magnet. The reaction was then continued for the rest of time (up to 45 min). At the end of this period only 46% of the product was obtained and no considerable change in the concentration of residual indole was observed according to the GC analysis of the reaction mixture.

4. CONCLUSION

In conclusion, we have developed a convenient method for one-pot three component reaction of indoles, phenylglyoxal monohydrate and *N*-arylenaminones under mild conditions. Highlights of the present work are regioselective one-pot formation of two C-C and one C-N bonds in a smooth cascade fashion, ease of recycling of the Fe_3O_4@MCM-41-OSO_3H catalyst which promises minimization of the waste, ease of work-up and more efficiency in terms of solvent, temperature and yield.

ACKNOWLEDGEMENT

The authors are grateful to the Research Council of University of Guilan for partial support of this study.

REFERENCES

1. Bandini, M., Eichholzer, A. (2009). "Catalytic Functionalization of Indoles in a New Dimension", *Angewandte Chemie International Edition,* 48**:** 9608-9644.
2. Humphrey, G. R., Kuethe, J. T. (2006). "Practical Methodologies for the Synthesis of Indoles", *Chemical Reviews,* 106**:** 2875-2911.
3. Zhang, H. -C., Ye, H., Moretto, A. F., Brumfield, K. K., Mnoff, B. E. (1999). "Facile Solid-Phase Construction of Indole Derivatives Based on a Traceless, Activating Sulfonyl Linker", Organic Letters, 2: 89-92.
4. Fernandez, L. S., Jobling, M. F., Andrews, K. T., Avery, V. M. (2008). "Antimalarial activity of natural product extracts from Papua New Guinean and Australian plants against Plasmodium falciparum", *Phytotherapy Research,* 22**:** 1409-1412.

5. Leclerc, S., Garnier, M., Hossel, R., Marko, D., Bibb, J. A., Snyder, G. L., Greengard, P., Biernat, J., Wu, Y. -Z., Mandelkow, E. -M., Eisenbrand, G., Meijer, L. (2001). "Indirubins Inhibit Glycogen Synthase Kinase-3β and CDK5/P25, Two Protein Kinases Involved in Abnormal Tau Phosphorylation in Alzheimer's Disease: A PROPERTY COMMON TO MOST CYCLIN-DEPENDENT KINASE INHIBITORS?", *Journal of Biological Chemistry,* 276**:** 251-260.
6. Adachi, J., Mori, Y., Matsui, S., Takigami, H., Fujino, J., Kitagawa, H., Miller, C. A., Kato, T., Saeki, K., Matsuda, T. (2001). "Indirubin and Indigo Are Potent Aryl Hydrocarbon Receptor Ligands Present in Human Urine", *Journal of Biological Chemistry,* 276**:** 31475-31478.
7. Shiri, M., Zolfigol, M. A., Kruger, H. G., Tanbakouchian, Z. (2009). "Bis- and Trisindolylmethanes (BIMs and TIMs)", *Chemical Reviews,* 110**:** 2250-2293.
8. Jiang, B., Feng, B. -M., Wang, S. -L., Tu, S. -J., Li, G. (2012). "Domino Constructions of Pentacyclic Indeno[2,1-c]quinolines and Pyrano[4,3-b]oxepines by [4+1]/[3+2+1]/[5+1] and [4+3] Multiple Cyclizations", *Chemistry – A European Journal,* 18**:** 9823-9826.
9. Jiang, B., Yi, M. -S., Shi, F., Tu, S. -J., Pindi, S., Mcdowell, P., Li, G. (2012). "A multi-component domino reaction for the direct access to polyfunctionalized indolesvia intermolecular allylic esterification and indolation", *Chemical Communications,* 48**:** 808-810.
10. Jiang, B., Yi, M.-S., Tu, M.-S., Wang, S.-L., Tu, S.-J. (2012). "Brønsted Acid-Promoted Divergent Reactions of Enaminones: Efficient Synthesis of Fused Pyrroles with Different Substitution Patterns", *Advanced Synthesis & Catalysis,* 354**:** 2504-2510.
11. Khorshidi, A. (2012). "Indole cyanation via CH bond activation under catalysis of Ru(III)-exchanged NaY zeolite (RuY) as a recyclable catalyst", *Chinese Chemical Letters,* 23: 903-906.
12. Khorshidi, A. (2012). "Ultrasound assisted, ruthenium-exchanged FAU-Y zeolite catalyzed alkylation of indoles with epoxides under solvent free conditions", *Ultrasonics Sonochemistry,* 19**:** 570-575.
13. Khorshidi, A., Tabatabaeian, K. (2011). "Ruthenium-exchanged FAU-Y zeolite catalyzed improvement in the synthesis of 6H-indolo[2,3-b]quinolines", *Journal of Molecular Catalysis A: Chemical,* 344**:** 128-131.
14. Fu, L. -P., Shi, Q. -Q., Shi, Y., Jiang, B., Tu, S. -J. (2013). "Three-Component Domino Reactions for Regioselective Formation of Bis-indole Derivatives", *ACS Combinatorial Science,* 15**:** 135-140.
15. Amrollahi, A., Hamidi, A. A., Rashidi, A. M. (2007). "Preparation of MCM-41 nanofluid and an investigation of Brownian movement of the nanoparticles on the nanofluid conductivity", *International Journal of Nanoscience and Nanotechnology,* 3: 13-20.
16. Masoumi, M., Mehrnia, M. R., Montazer-Rahmati, M. M., Rashidi, A. M. (2010). "Templated Growth of Carbon Nanotubes on Nickel Loaded Mesoporous MCM-41 and MCM-48 Molecular Sieves", *International Journal of Nanoscience and Nanotechnology,* 6: 88-96.
17. Keyhanian, F., Shariati, S., Faraji, M., Hesabi, M. (2011). "Magnetite nanoparticles with surface modification for removal of methyl violet from aqueous solutions", *Arabian Journal of Chemistry*.
18. Kiasat, A. R., Davarpanah, J. (2013). "Fe_3O_4@silica sulfuric acid nanoparticles: An efficient reusable nanomagnetic catalyst as potent solid acid for one-pot solvent-free synthesis of indazolo[2,1-b]phthalazine-triones and pyrazolo[1,2-b]phthalazine-diones", *Journal of Molecular Catalysis A: Chemical,* 373**:** 46-54.
19. Jang, J. H., Lim, H. B. (2010). "Characterization and analytical application of surface modified magnetic nanoparticles", *Microchemical Journal,* 94: 148-158.
20. Kim, J. M., Kwak, J. H., Jun, S., Ryoo, R. (1995). Ion exchange and thermal stability of MCM-41", *The Journal of Physical Chemistry,* 99: 16742-16747.